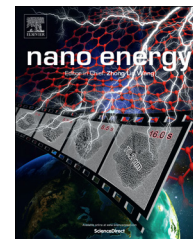




Available online at www.sciencedirect.com

ScienceDirect

journal homepage: www.elsevier.com/locate/nanoenergy



RAPID COMMUNICATION

Surface plasmon resonance enhanced highly efficient planar silicon solar cell



Lin-Bao Luo^{a,*}, Chao Xie^{a,**}, Xian-He Wang^a, Yong-Qiang Yu^a,
Chun-Yan Wu^a, Han Hu^a, Ke-Ya Zhou^{b,***}, Xi-Wei Zhang^c,
Jian-Sheng Jie^{c,****}

^aSchool of Electronic Science and Applied Physics and Anhui Provincial Key Laboratory of Advanced Functional Materials and Devices, Hefei University of Technology, Hefei, Anhui 230009, PR China

^bDepartment of Physics, Harbin Institute of Technology, Harbin, Heilongjiang 150001, PR China

^cInstitute of Functional Nano & Soft Materials (FUNSOM), Jiangsu Key Laboratory for Carbon-Based Functional Materials & Devices, Soochow University, Suzhou, Jiangsu 215123, PR China

Received 12 March 2014; received in revised form 12 June 2014; accepted 8 July 2014

Available online 24 July 2014

KEYWORDS

Plasmonic nanoparticles;
Photovoltaic devices;
Graphene;
Light harvesting;
Finite element method

Abstract

Metal nanoparticles (NPs) induced surface plasmon resonance (SPR) is of great interest for efficient controlling over light's propagation and absorption in optoelectronic devices applications. In this work, we proposed a simple strategy to improve the photocurrent of planar silicon (Si) *p-n* junction solar cells by attaching plasmonic Au nanoparticles (AuNPs) onto transparent graphene film to enhance incident light harvesting. Finite Element Method based simulations reveal that the strong light scattering by AuNPs is responsible for the optical absorption enhancement within Si, leading to the increase in photocurrent. In addition, decoration of AuNPs on graphene also contributes to a high fill factor (*FF*) by reducing series resistance in the circuit. These contributory factors, together with the effective surface passivation of Si yield a power conversion efficiency (PCE) as high as 10.15%, with excellent reproducibility. This study will open up new opportunities for the optimization of Si based optoelectronic devices.

© 2014 Elsevier Ltd. All rights reserved.

*Corresponding author. Tel.: +86 551 62901993.

**Corresponding author. Tel.: +86 551 62902064.

***Corresponding author. Tel.: +86 13633611093.

****Corresponding author. Tel.: +86 512 65881265.

E-mail addresses: luolb@hfut.edu.cn (L.-B. Luo),
shieh.chaoxie@mail.hfut.edu.cn (C. Xie),
zhoukeya@hit.edu.cn (K.-Y. Zhou), jsjie@suda.edu.cn (J.-S. Jie).

Introduction

Plasmonic metal nanoparticles (NPs) have recently stimulated increasing research interest for advanced light trapping management in various fields because they can be used as subwavelength scattering elements, to couple and trap

freely propagating plane waves from the sun into an absorbing semiconductor layer, causing an increase in the effective optical path length in the semiconductor [1,2]. Extensive study has demonstrated that it is feasible to engineer the metal NPs structure to maximize the scattering and minimize the absorption in metal NPs across the wavelength range of interest in optoelectronic devices [3-5]. By this token, plasmonic light management has been widely applied to various optoelectronic devices such as lasers [6,7], light-emitting diodes [8,9], photodetectors [10,11], and solar cells [12,13]. Metal NPs with strong light scattering properties and local electric field enhancement can increase light absorption within semiconductor materials, leading to enhanced photocurrents and therefore improved device performance [14]. For example, Schaadt and co-workers observed enhanced optical absorption and photocurrent in silicon (Si) *p-n* photodiodes induced by scattering from surface plasmon resonance (SPR) when Au nanoparticles (AuNPs) were deposited on the photodiodes surface [15]. Nakayama et al. reported on the fabrication of optically thin GaAs solar cells decorated with size-controlled Ag nanoparticles (AgNPs) [16]. The photocurrent of the solar cells was increased by 8% as a result of the strong scattering by the interacting surface plasmons in high aspect-ratio AgNPs.

Si as the leading material in commercial solar cell modules accounts for more than 90% of the global photovoltaic market. Traditional wafer-based Si solar cells normally employ metal grids or indium tin oxide (ITO) as top electrodes. Nevertheless, the metal grids usually cover 5-20% of the surface area of the solar cells, which means some of the incident light would not arrive at the *p-n* junction [17]. On the other hand, ITO has its own problems such as the scarcity, high cost of indium, the non-flexibility as well as relatively inferior optical transmittance. In light of this, people recently resort to graphene with higher optical transmittance, lower sheet resistance, outstanding mechanical flexibility and excellent chemical/thermal stability [18,19]. Graphene as transparent electrode has found wide application in Si based photovoltaic devices, including graphene/Si nanostructures [20-22], graphene/Si substrate junction [23,24], and so on. In spite of these tremendous progresses, there are still some drawbacks in current graphene/Si solar cells research that impedes their wide applications: (1) the inherent disadvantages of Schottky-type solar cells such as severe interface diffusion/reaction and the large current leakage originating from the small work difference [25]. (2) Poor device stability in air due to volatile oxidants such as HNO₃ and SOCl₂ widely used in previous studies to reduce the sheet resistance of graphene. Without question, these factors will increase the device complexity and cause serious degradation of the device stability/reproducibility. Herein, we propose a new strategy to improve the PCE of planar Si *p-n* junction solar cells by decorating AuNPs with strong SPR onto the transparent graphene. Device analysis reveals that after AuNPs decoration, the PCE was improved from 6.39% to 10.15%. Theoretical simulation based on the Finite Element Method (FEM) reveals that the improvement in photocurrent is associated with the enhancement of light absorption within Si substrate as a result of the strong light scattering by AuNPs. In addition, decoration of AuNPs on graphene also contributes

to a high fill factor (*FF*) by reducing series resistance in the circuit.

Results and discussion

The scheme in Figure 1(a) illustrates the procedures to fabricate the planar Si *p-n* junction solar cells with AuNPs decorated graphene as transparent electrodes. The detailed fabrication process was included in Experimental section. Figure 1(b) depicts the scanning electron microscopy (SEM) image of AuNPs on graphene films. Transmission electron microscopy (TEM) of a typical AuNP in the inset of Figure 1(b) indicates that the AuNPs have sphere-like morphology. According to the statistical distribution in Figure 1(c), the typical diameters of these spherical AuNPs are in the range of 40-100 nm, with an average diameter of ~65 nm. Further X-ray photoelectron spectroscopy (XPS) of AuNPs on 4-layer few layers graphene (FLG) films in Figure 1(d) shows four peaks in the Au 4f spectrum: two Au³⁺ related peaks near 90.88 and 87.28 eV and two Au⁰ peaks near 88.18 and 84.38 eV, respectively. The AuNPs are understandably formed as Au ions can be reduced to neutral Au atoms by accepting electrons from graphene [26]. Interestingly, such a chemical reaction can not only result in the formation of plasmonic Au nanoparticles with strong SPR, but also lead to increased hole concentration in graphene. This case is different from the 'percolation doping' of graphene, in which metal nanowire network decorating on top of/below graphene layers can provide conduction channels across the grain boundaries, reducing the sheet resistance of graphene layers [27]. Such a *p*-type doping [28], with obvious decrease in sheet resistance after surface decoration (see Table S1), was also verified by the Raman spectroscopy analysis in Figure 1(e): due to the phonon stiffening effect by charge extraction, the G band position slightly shifts from 1851.7 to 1856.4 after AuNPs decoration [29]. It is worth noting that after AuNPs decoration, the 2D-band to G-band intensity ratio (*I*_{2D}:*I*_G) increases from ~3.87 to ~4.71, suggesting that original monolayer graphene films have high crystal quality, and AuNPs decoration on graphene films does not destroy their quality [30].

In this study, the layer number of graphene films was optimized to be 4 layers considering the tradeoff of optical transmittance and electrical conductivity [31]. Figure 2(a) plots a typical current versus voltage (*I-V*) curve of a typical planar Si *p-n* junction with 4-layer FLG transparent electrode without decoration which exhibits an excellent rectification behavior with a high rectification ratio of 1.7×10^3 within ± 0.8 V and a low turn-on voltage of ~0.43 V. This rectifying characteristics shall not arise from *p*-Si/graphene considering the factor that graphene can form good contact with *p*-Si substrate (Figure S1). From the dark ln *I-V* curve in the inset of Figure 2(a), the diode ideality factor (*n*) is estimated to be 1.82, smaller than that of Si nanowire radial *p-n* junction (2.1) [32], this relatively low ideal factor suggests a lower interface recombination in present device [33]. Figure 2(b) presents the photovoltaic characteristics of planar Si *p-n* junction solar cell with 4-layer FLG transparent electrode under AM 1.5G light irradiation. Apparently, this device exhibits pronounced photovoltaic properties, with an open-circuit voltage (*V*_{oc})

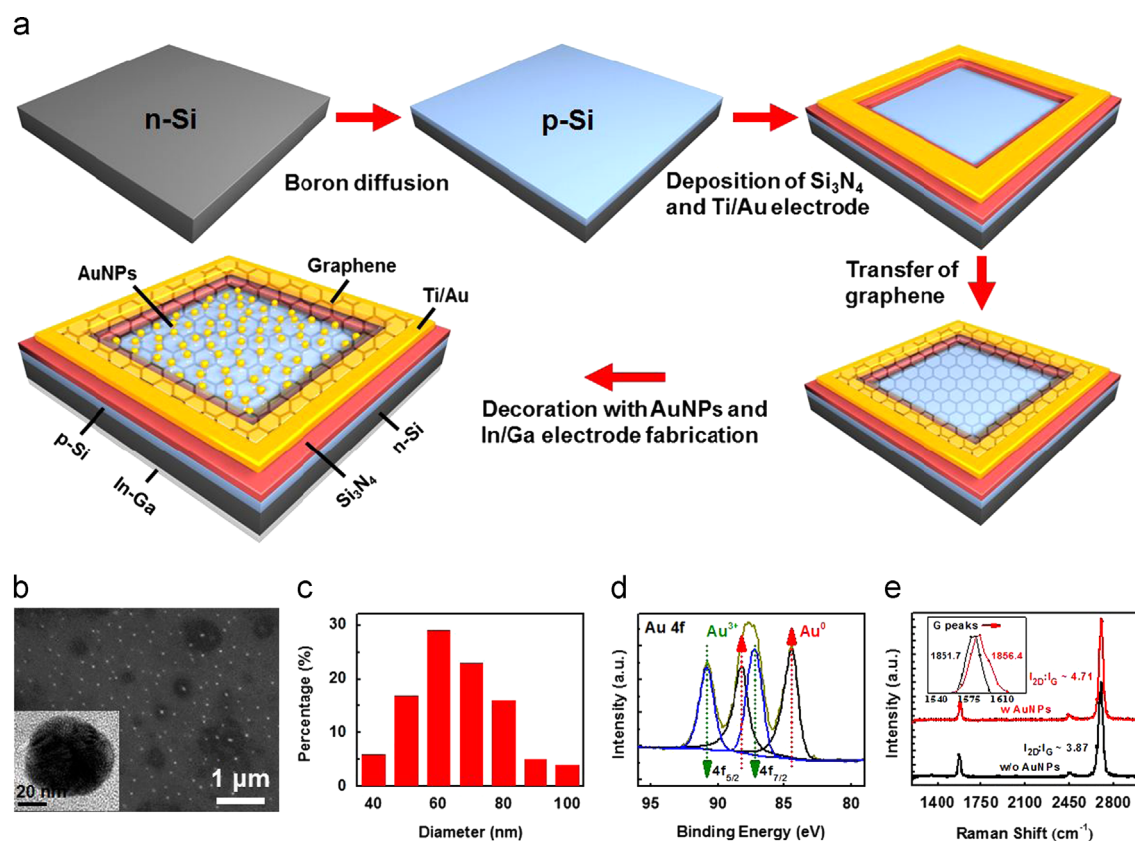


Figure 1 (a) Schematic illustration of step-wise process for the fabrication of planar Si *p-n* junction solar cell with AuNPs decorated graphene. (b) SEM image of AuNPs on graphene, the inset shows a TEM image of a typical AuNP. (c) Statistical distribution of the diameter of AuNPs. (d) XPS spectrum of AuNPs. (e) Raman spectra of the 4-layer FLG with and without AuNPs.

of 502 mV, a short circuit current density (J_{SC}) of 26.84 mA cm⁻², a fill factor (FF) of 0.474, yielding a PCE of 6.39%. Notably, upon decoration of AuNPs atop graphene electrode, the device photovoltaic performance increases dramatically. The V_{OC} slightly increases to 521 mV, while the J_{SC} and FF increase substantially to 31.63 mA cm⁻² and 0.616, respectively, giving rise to a PCE of 10.15%. Significantly, such SPR enhanced high performance is highly reproducible. Figure 2(c) compares the PCEs of 14 representative photovoltaic devices with and without surface functionalization, from which, it is seen that after decoration of plasmonic AuNPs, all the devices enjoy substantial increase in PCE, with average value from 6.15% to 9.82%. This reliable characteristic is important for their practical application.

Two factors are considered crucial to the improved device performance: first, reduced reflectance of the solar cell. As illustrated in Figure 2(d), after AuNPs decoration, the reflectance of the device was reduced by 5-11% in the wavelength from 400 to 1000 nm, which is highly beneficial to the device performance. Figure 2(e) compares the external quantum efficiency (EQE) curves of the solar cell with and without AuNPs. The obvious higher EQE value after decoration suggests more efficient light harvesting and carrier transfer/collection in the solar cell, leading to a large J_{SC} value. Second, the reduce in sheet resistance of the graphene. As mentioned above, the AuNPs doping can cause a decrease in series resistance (R_s) in the circuit, while the parallel resistance (R_p) remains unchanged

(Figure 2(b)). Therefore, the smaller R_s would lead to a higher FF and be favorable to a higher J_{SC} [34].

In order to elucidate the physical mechanisms of the photovoltaic performance promotion after AuNPs decoration, we adopted the FEM to simulate the optical properties of the constructed structures. The model is composed of an infinite Si substrate in close contact with 4-layer FLG, on which AuNPs are on the surface. The density and size of AuNPs are determined by the lattice constant l and the AuNP diameter d , respectively (Figure 3(a)). The optical constants of Si and Au are obtained from previous literature using a linear interpolation method [35]. To illustrate the optical constant of 4-layer FLG, we use the σ_0 model, in which the optical constants are calculated as [36]

$$n = \text{Re}\{\sqrt{\varepsilon_\sigma}\}, \quad k = \text{Im}\{\sqrt{\varepsilon_\sigma}\}$$

with the dielectric constant

$$\varepsilon_\sigma = 1 + \frac{i\sigma_0}{\omega\varepsilon_0 d_g}$$

where $d_g = 0.335$ nm is the thickness of a graphene layer, ω is the light frequency, and ε_0 is the vacuum permittivity, σ_0 is the optical sheet conductivity $\sigma_0 = e^2/4\hbar$.

We in total studied 3 samples with different parameters: Sample A ($l=400$ nm, $d=60$ nm), Sample B ($l=400$ nm, $d=80$ nm) and Sample C ($l=300$ nm, $d=80$ nm). For clarity, samples without AuNPs were considered as well. From the reflectance spectrum in Figure 3(b), it is observed that the

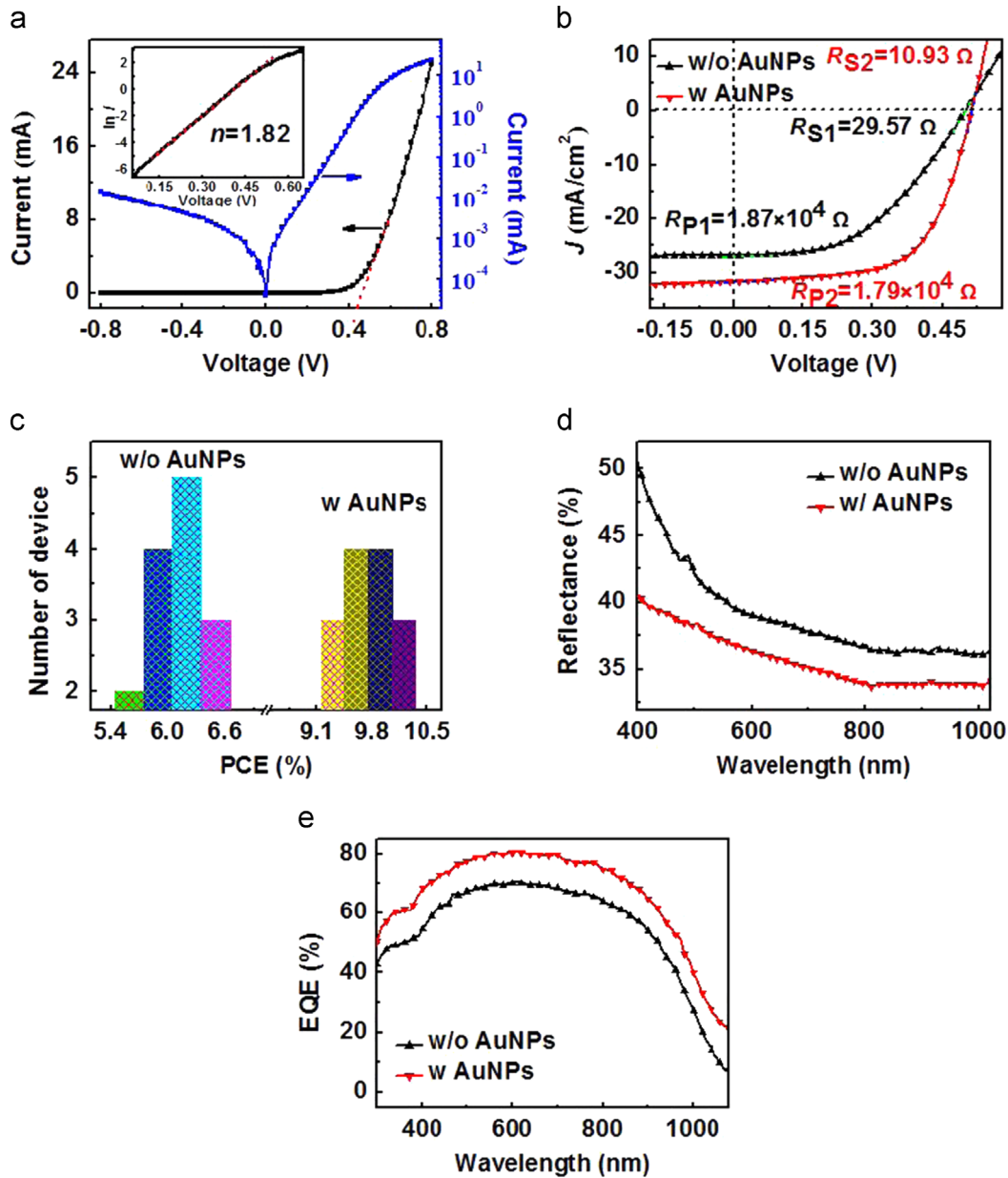


Figure 2 (a) I - V curve of the planar Si p - n junction with 4-layer FLG without AuNPs decoration, the inset plots the $\ln I$ - V curve from which the ideality factor of the planar Si p - n junction is estimated. (b) Photovoltaic characteristics of the planar Si p - n junction device before and after AuNPs decoration. (c) PCEs of 14 representative solar cells before and after decoration with AuNPs. (d) and (e) Reflectance and EQE spectra of 4-layer FLG on planar Si substrate with and without AuNPs decoration.

reflectance of all three samples was reduced after decoration of AuNPs, in consistence with the experimental result mentioned above. Moreover, among the three samples, Sample C has the lowest reflectance due to its higher particle density and larger sizes. That is to say, AuNPs with higher density and larger size could result in a lower reflectance in the whole spectrum. In addition to reflectance, the functionalization of AuNPs can increase the absorption of Si substrate and FLG (see Figure 3(c and d)). Remarkably, for all absorption spectra of Si substrate, an absorption peak at ~ 520 nm due to the plasmonic resonance of AuNPs was observed. As for wavelengths larger than 520 nm, the in phase transmitted plane wave and scattered wave result in an even higher absorption enhancement than lower wavelengths. The lower absorption in a

spectrum below 520 nm is partially due to the out of phase scattered light and partly caused by the high Joule loss in AuNPs. It is worth noting that the optical loss in 4-layer FLG is far less than the monolayer graphene's opacity ($\pi\alpha=2.3\%$, dashed line in the inset of Figure 3(d)) for all three samples. This is because the 4-layer FLG is in direct contact with Si substrate, which results in a completely different boundary condition from the case of freestanding monolayer graphene. This fact signifies that the optical loss of $<2\%$ in the 4-layer FLG could be neglected for its application in solar cell as transparent electrode.

To unveil the enhancement effect of AuNPs on the light absorption in Si substrate, we simulated the relative electric field distribution ($|E|^2/|E_0|^2$) by using two different

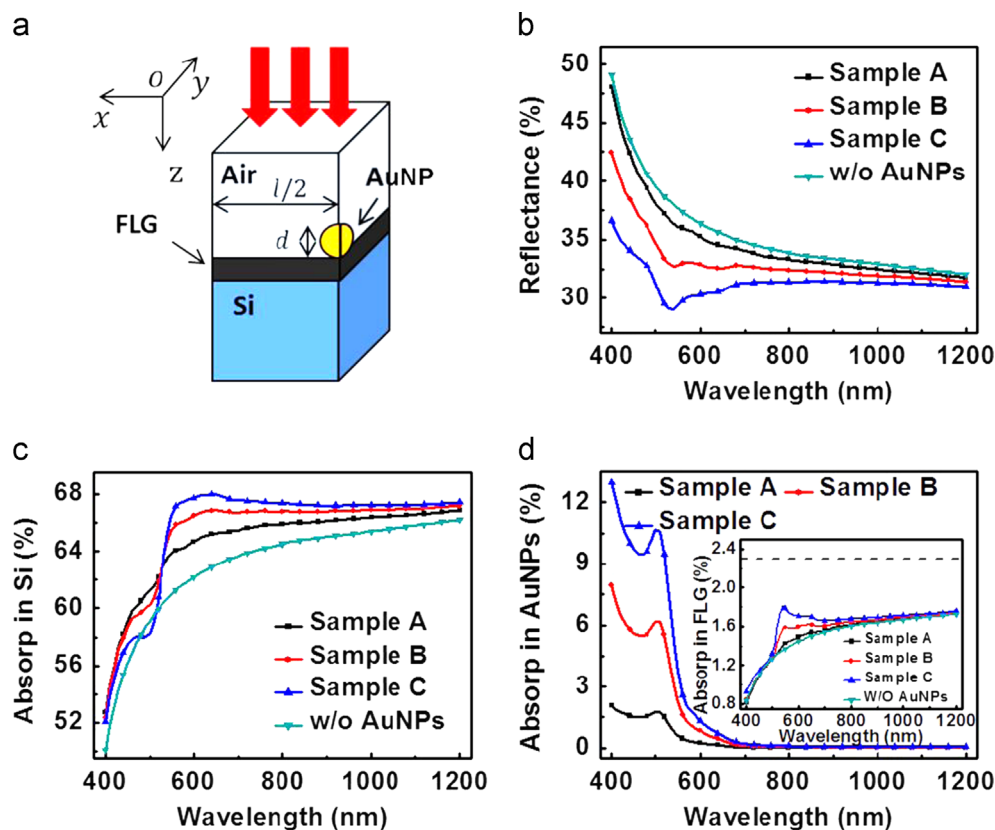


Figure 3 (a) Schematic diagram of simulation geometry employed. Simulated reflectance (b), absorption in Si substrate (c) and absorption in AuNPs (d) of proposed sample A ($l=400$ nm, $d=60$ nm), sample B ($l=400$ nm, $d=80$ nm), sample C ($l=300$ nm, $d=80$ nm) and the sample without decoration of AuNPs, the inset of (d) shows the absorption in 4-layer FLG.

kinds of incident light (600 and 1000 nm). At wavelength of 600 nm which is close to SPR wavelength of AuNPs, the relative refractive index (RI) of Si is $n-j\kappa=3.95-0.026j$. Considering the employment of FLG, the energy transmitted into Si substrate is around 62.2% (see Figure 4(a)). As the absorption coefficient of Si is calculated to be $\alpha=4\pi\kappa/\lambda=0.54\ \mu\text{m}^{-1}$, a rapid decrease of electric field in Si substrate is seen along the direction of incident light. Upon decoration of plasmonic nanoparticles, obvious hot spots with high field intensity due to SPR scattering effect are apparently observed beneath the AuNPs. The overall absorption enhancement in Si substrate are calculated to be 2.5, 4.3 and 5.5% for Samples A, B and C, respectively. With regard to the incident light with wavelength of 1000 nm, the relative RI of Si is $n-j\kappa=3.6-0.003j$. The low absorption coefficient $\alpha=4\pi\kappa/\lambda=0.038\ \mu\text{m}^{-1}$ results in an almost unchanged electric field distribution in Si substrate as shown in Figure 4(e). It is worth noting that the electric field inside the AuNP is almost zero in Figure 4(e)-(h), and the scattered light is slightly affected by the AuNPs. This simulation result confirmed that the SPR of AuNPs takes a positive role on light absorption enhancement in such nanostructures. In addition, the introduction of FLG hardly influenced the optical properties of the proposed geometries. The theoretical study confirms the presence of SPR effect: strong light scattering of AuNPs and increased local electric field amplitude in Si, which can contribute to the absorption enhancement within Si substrate, leading to increased photocurrent in the solar cells.

In order to verify how the diameter and density of the NPs will influence the optical properties as well as device performance, two kinds of AuNPs with uniform diameter of ~ 60 and 80 nm (see Figure S3) were synthesized via a new method [37], which is good at precisely controlling the size of AuNPs. Based on these AuNPs, we fabricated three more devices marked as sample 1, sample 2 and sample 3, corresponding to the sample A (lattice constant $l=400$ nm, AuNP diameter $d=60$ nm), sample B ($l=400$ nm, $d=80$ nm) and sample C ($l=300$ nm, $d=80$ nm). Figure S4(a) shows the optical property of the three samples, from which, one can see that compared with sample 1, samples 2 exhibits lower reflectance in the wavelength from 400 to 1000 nm. What is more, compared with 2, sample 3 shows lower reflectance. These results are in good consistence with the previous simulation results. Figure S4(b) shows the electrical performance of the three samples, from which it can be seen that the short-current densities are 28.56, 29.38 and 30.14 mA/cm² for sample 1, sample 2 and sample 3, respectively. Thus it can be concluded that larger AuNPs size and density is beneficial to power conversion efficiency.

The air stability of a solar cell is critical for its practical application. Volatile oxidants such as HNO₃ and SOCl₂ were widely used in previous studies to reduce the sheet resistance of graphene films. [21,38]. Though pronounced the effect of these volatile oxidants is, it is not air stable. In contrast to the volatile oxidants, AuCl₃ proves to be a relatively stable dopant for graphene due to its nonvolatile property and the hygroscopic of Cl⁻ ions [39]. Figure 5

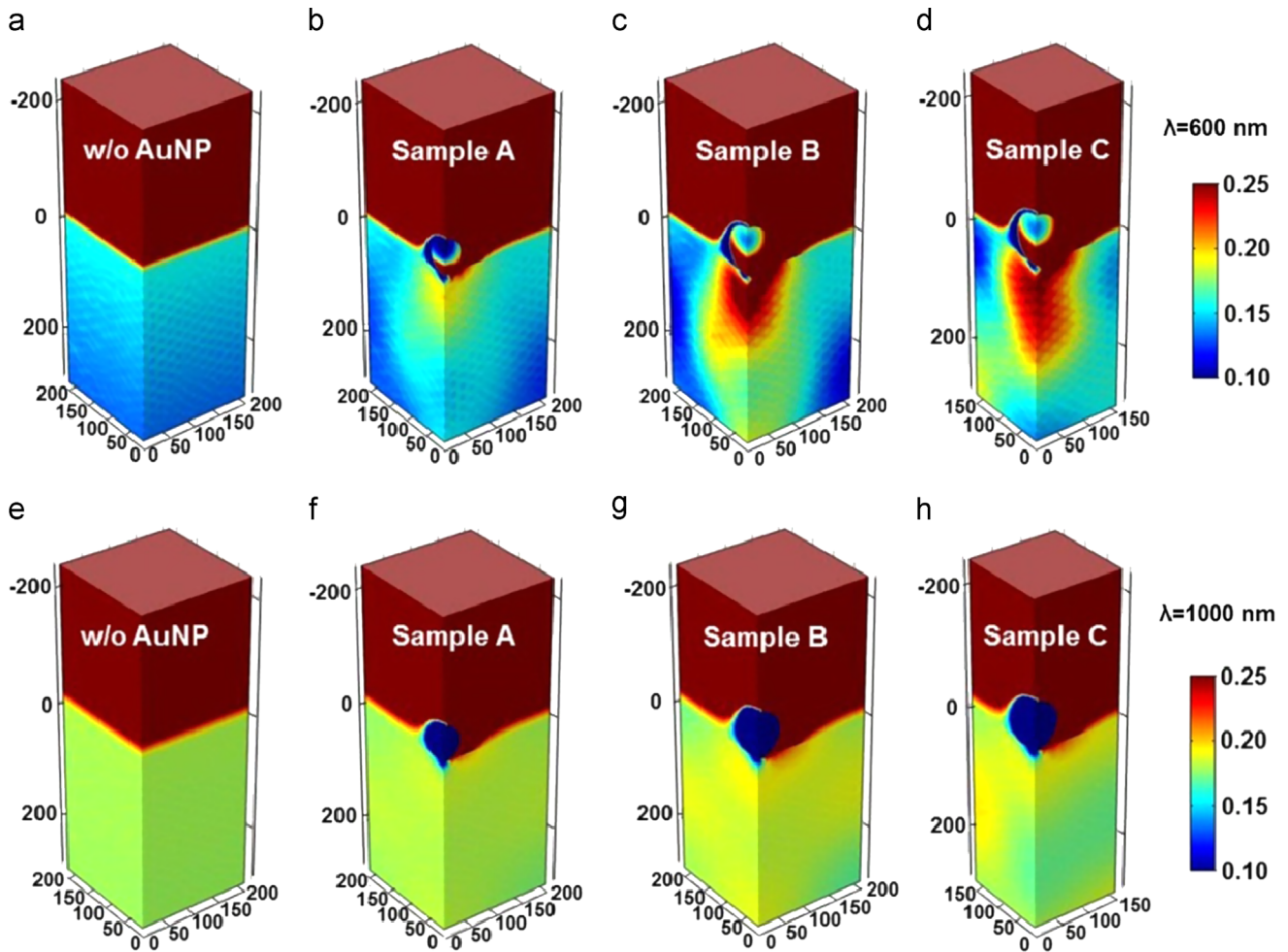


Figure 4 (a)-(d) Electric field distribution at wavelength of 600 nm for Sample without AuNP, Sample A, B and C. (e)-(f) Electrical field distribution at wavelength of 1000 nm for Sample without AuNP, Sample A, B and C.

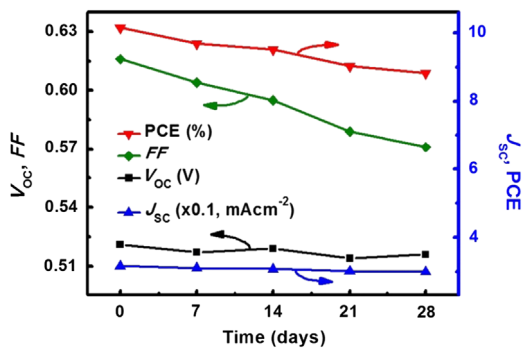


Figure 5 Plots of V_{oc} , J_{sc} , FF and PCE of the planar Si p - n junction solar cell with AuNPs decorated 4-layer FLG as function of storage time.

(a) shows the air stability of the planar Si p - n junction solar cell with AuNPs decorated graphene as a function of storage duration. It is seen that the both V_{oc} and J_{sc} keep nearly identical, while the FF decreases from 0.616 to 0.571, resulting in a reduced PCE of 8.82%, about 87% of the original value (10.15%). The slight degradation of the FF can be probably attributed to the increased R_s in circuit as a

result of the reduced sheet conductivity of graphene over time [26]. Note that the photovoltaic device in our work is more stable than previously reported volatile acids doped graphene/Si solar cells [37], indicative of the great potential for graphene based optoelectronic devices applications.

Conclusion

In summary, we reported on the fabrication of highly efficient planar Si p - n junction solar cells with AuNPs decorated graphene transparent electrodes and the PCE of the solar cells was improved from 6.39% to 10.15% by using a simple surface modification strategy. Theoretical simulation results reveal that the improvement in photocurrent is mainly attributed to the enhancement of light absorption within Si substrate as a result of the strong light scattering by AuNPs. Meanwhile, the reduced sheet resistance of graphene electrode because of the decoration of AuNPs is responsible for the improved FF. At last, the air stability of the solar cell was studied, revealing the potential of present photovoltaic devices in practical applications. The experimental and simulation results here are believed helpful for the future optimization of Si and graphene based photovoltaic devices.

Experimental section

Preparation and surface passivation of planar Si *p-n* junction

The *p-n* junction was fabricated by a thermal boron (B) diffusion process. Briefly, *n*-type Si (100) wafer with resistivity of 1–10 Ω cm and thickness of 500 μ m was first washed by sonication in acetone and deionized water and dried by a steam of N_2 . To form *p-n* junction, B atoms were diffused into the wafer at 920 $^\circ$ C for 40 min using high purity BN wafer as B source under N_2 protection in tube furnace. After diffusion, the wafer was immersed into a diluted HF solution for 3 min to remove borosilicate glass formed in the diffusion process, followed by rinse with deionized water. The sheet resistance of the resulting *p*-type layer was \sim 90 Ω per square, and based on the above process parameters, the junction depth was estimated to be \sim 0.3 μ m [40]. To passivate the surface, the above *p-n* junction was immersed into an HF solution (5 M) with gentle shaking for 10 min, followed by cleaning in deionized water and drying by N_2 . The as-obtained H-Si substrate was then immediately transferred into a glovebox, in which methyl-terminated Si surface was prepared by using a two-step chlorination/alkylation process [41].

Preparation and characterization of graphene

Monolayer graphene (MLG) films were prepared on Cu substrates at 1000 $^\circ$ C *via* a chemical vapor deposition (CVD) method [42]. After growth, polymethylmethacrylate (PMMA, 5 wt% in chlorobenzene) was spin-coated on the as-prepared MLG films and the underlying Cu foils were etched away in Marble's reagent solution ($CuSO_4:HCl:H_2O=10$ g:50 ml:50 ml). The resultant MLG films were cleaned in deionized water for several times and ready for use. The MLG film was directly transferred onto SiO_2/Si substrate and the PMMA was removed by acetone. The morphology and structure of the AuNPs on graphene were characterized by scanning electron microscopy (SEM, FEI/Quanta 200 FEG) and transmission electron microscopy (TEM, FEI Tecnai G2 F20 S-TWIN). The chemical composition of the AuNPs on graphene was analyzed by X-ray photoemission spectroscopy (XPS) which was performed on a VG ESCALAB 220i-XL surface analysis system equipped with a monochromatic Al X-ray (1486.6 eV) source. The pristine 4-layer FLG and the AuNPs decorated 4-layer FLG were characterized by a Raman spectroscopy (Jobin Yvon/Labram HR800, 633 nm) with a beam size of 2 μ m.

Construction and evaluation of the solar cells

Reactive ion etching (RIE) technology was firstly employed for 5 min to remove the *p-n* junction formed in the rear. To fabricate the solar cells, a 300 nm Si_3N_4 insulating layer was deposited onto the diffused Si wafer using magnetron sputtering and the wafer was cut into small substrates (1.5 \times 1.5 cm^2). Opening window (4 \times 4 mm^2) was defined on the substrate by adhesive tape and then the Si_3N_4 insulating layer in the opening window was removed by a buffered oxide etch (BOE) solution. After that, Ti/Au (5/50 nm) electrode, serving as the electrical contact for

graphene, was deposited on the Si_3N_4 layer nearby the exposed Si window *via* electron-beam deposition. The PMMA-supported MLG film was then transferred onto the substrate and dried at 100 $^\circ$ C for 10 min, followed by remove the PMMA in acetone. Devices with 4-layer FLG films were prepared by repeating the transfer process for 4 times. Eventually, indium-gallium (In-Ga) alloy was adhered to the rear of *n*-Si substrate to form ohmic contact to the *n*-Si. AuNPs on graphene was obtained by spin-coating of $AuCl_3$ (10 mM in nitromethane) onto the substrate at 2000 rpm for 1 min. The photovoltaic characteristics of the solar cells were evaluated by a Keithley 2612 source meter in ambient environment. Newport 91160 solar simulator equipped with a 300 W xenon lamp and an air mass (AM) 1.5 filter was employed to generate simulated AM 1.5G solar irradiation (100 mW cm^{-2}).

Simulations using Finite element method (FEM)

For simulation of the considered model, the incident light is set to be an *x*-polarized plane wave propagating along $-z$ axis. Boundary conditions of perfect magnetic conductors (PMCs) were used for $y=0$ and $y=l/2$ planes, and perfect electric conductors (PECs) conditions were used for the other two planes, $x=0$ and $x=l/2$. Perfect matched layers (PMLs) were used at the top and bottom of the unit cell and ended with the scattering boundaries. The total reflectance of the system is determined by the integration

$$R = 1 - \frac{\iint P_z dx dy}{E_{in}}$$

in which P_z is the averaged power flow in a probe plane in front of the cell and E_{in} is the total energy of the incident light into the considered cell.

To illustrate the optical loss in AuNPs and 4-layer FLG, we adopted the volume integration over the selective region

$$LOSS = \frac{\iiint Q_e dV}{E_{in}} = \frac{\iiint 0.5\omega\epsilon_0\epsilon''|E|^2 dV}{E_{in}}$$

in which Q_e is the electromagnetic power loss density, ω is the light angular frequency, ϵ_0 is the dielectric constant, E is the electric field and ϵ'' is the imaginary part of the relative dielectric constant. For Au and Si, we adopted the values of relative dielectric constants from a reference [43]. As for 4-layer FLG, we adopted the σ_0 model, and its wavelength dependent optical constants (*n* and *ki*) of 4-layer FLG are shown in Figure S2.

The light absorption in Si substrate is calculated by the following expression

$$A_{Si} = 1 - R - LOSS_{AuNP} - LOSS_{FLG}$$

Acknowledgments

This work was supported by the Natural Science Foundation of China (NSFC, Nos. 21101051, 51172151, 61106010, 61308017), the Fundamental Research Funds for the Central Universities (Nos. 2013HGXJ0195, 2013HGCH0012, HIT.NSRIF.2011015), and the Major Research Plan of the National Natural Science Foundation of China (No. 91233110).

Appendix A. Supporting information

Supplementary data associated with this article can be found in the online version at <http://dx.doi.org/10.1016/j.nanoen.2014.07.003>.

Reference

- [1] H.A. Atwater, A. Ploman, *Nat. Mater.* 9 (2010) 205.
- [2] S. Pillai, M.A. Green, *Sol. Energy Mater. Sol. Cells* 94 (2010) 1481.
- [3] K.R. Catchpole, A. Polman, *Opt. Express* 16 (2008) 21793.
- [4] K.R. Catchpole, A. Polman, *Appl. Phys. Lett.* 93 (2008) 191113.
- [5] C.F. Bohren, D.R. Huffman, *Absorption and Scattering of Light by Small Particles*, Wiley-VCH, Weinheim, 2004.
- [6] R.F. Oulton, V.J. Sorger, T. Zentgraf, R.M. Ma, C. Gladden, L. Dai, G. Bartal, X. Zhang, *Nature* 461 (2009) 629.
- [7] M.T. Hill, Y.S. Oei, B. Smalbrugge, Y.C. Zhu, T. De Vries, P.J. Van Veldhoven, F.W.M. Van Otten, T.J. Eijkemans, J.P. Turkiewicz, H. De Waardt, E.J. Geluk, S.H. Kwon, Y.H. Lee, R. Nötzel, M.K. Smmit, *Nat. Photonics* 1 (2007) 589.
- [8] M.K. Kwon, J.Y. Kim, B.H. Kim, I.K. Park, C.Y. Cho, C.C. Byeon, S.J. Park, *Adv. Mater.* 20 (2008) 1253.
- [9] K. Okamoto, I. Niki, A. Shvartser, Y. Narukawa, T. Mukai, A. Scherer, *Nat. Mater.* 3 (2004) 601.
- [10] M.W. Knight, H. Sobhani, P. Nordlander, N.J. Halas, *Science* 332 (2011) 702.
- [11] L.B. Luo, L.H. Zeng, C. Xie, Y.Q. Yu, F.X. Liang, C.Y. Wu, L. Wang, J.G. Hu, *Sci. Rep.* 4 (2014) 3914.
- [12] R.A. Pala, J. White, E. Barnard, J. Liu, M.L. Brongersma, *Adv. Mater.* 21 (2009) 3504.
- [13] D. Derkacs, S.H. Lim, P. Matheu, W. Mar, E.T. Yu, *Appl. Phys. Lett.* 89 (2006) 093103.
- [14] H.R. Tan, R. Santbergen, A.H.M. Smets, M. Zeman, *Nano Lett.* 12 (2012) 4070.
- [15] D.M. Schaadt, B. Feng, E.T. Yu, *Appl. Phys. Lett.* 86 (2005) 063106.
- [16] K. Nakayama, K. Tanabe, H.A. Atwater, *Appl. Phys. Lett.* 93 (2008) 121904.
- [17] Y.M. Chi, H.L. Chen, Y.S. Lai, H.M. Chang, Y.C. Liao, C.C. Cheng, S.H. Chen, S.C. Tseng, K.T. Lin, *Energy Environ. Sci.* 6 (2013) 935.
- [18] K.S. Kim, Y. Zhao, H. Jang, S.Y. Lee, J.M. Kim, K.S. Kim, J.H. Ahn, P. Kim, J.Y. Choi, B.H. Hong, *Nature* 457 (2009) 706.
- [19] K.C. Kwon, K.S. Choi, S.Y. Kim, *Adv. Funct. Mater.* 22 (2012) 4724.
- [20] C. Xie, P. Lv, B. Nie, J.S. Jie, X.W. Zhang, Z. Wang, P. Jiang, Z.Z. Hu, L.B. Luo, Z.F. Zhu, L. Wang, C.Y. Wu, *Appl. Phys. Lett.* 99 (2011) 133113.
- [21] Y.M. Wu, X.Z. Zhang, J.S. Jie, C. Xie, X.W. Zhang, B.Q. Sun, Y. Wang, P. Gao, *J. Phys. Chem. C* 117 (2013) 11968.
- [22] C. Xie, J.S. Jie, B. Nie, T.X. Yan, Q. Li, P. Lv, F.Z. Li, M. Z. Wang, C.Y. Wu, L. Wang, L.B. Luo, *Appl. Phys. Lett.* 100 (2012) 193103.
- [23] X.M. Li, H.W. Zhu, K.L. Wang, A.Y. Cao, J.Q. Wei, C.Y. Li, Y. Jia, Z. Li, X. Li, D.H. Wu, *Adv. Mater.* 22 (2010) 2743.
- [24] X.C. Miao, S. Tongay, M.K. Petterson, K. Berke, A.G. Rinzler, B.R. Appleton, A.F. Hebard, *Nano Lett.* 12 (2012) 2745.
- [25] H.J. Hovel, in: R.K. Willardson, A.C. Beer (Eds.), *Semiconductors and Semimetals: Solar Cells*, vol. 11, New York: Academic Press, New York, 1975.
- [26] F. Güneş, H.J. Shin, C. Biswas, G.H. Han, E.S. Kim, S.J. Chae, J.Y. Choi, Y.H. Lee, *ACS Nano* 4 (2010) 4595.
- [27] R.Y. Chen, S.R. Das, C.W. Jeong, M.R. Khan, D.B. Janes, M.A. Alam, *Adv. Funct. Mater.* 23 (2013) 5150.
- [28] Y.M. Shi, K.K. Kim, A. Reina, M. Hofmann, L.J. Li, J. Kong, *ACS Nano* 4 (2010) 2689.
- [29] A.M. Rao, P.C. Eklund, S. Bandow, A. Thess, R.E. Smalley, *Nature* 388 (1997) 257.
- [30] A. Reina, X.T. Jia, J. Ho, D. Nezich, H. Son, V. Bulovic, M.S. Dresselhaus, J. Kong, *Nano Lett.* 9 (2009) 30.
- [31] Y. Wang, S.W. Tong, X.F. Xu, B. Özyilmaz, K.P. Loh, *Adv. Mater.* 23 (2011) 1514.
- [32] E.C. Garnett, P.D. Yang, *J. Am. Chem. Soc.* 130 (2008) 9224.
- [33] Y. Jung, X.K. Li, N.K. Rajan, A.D. Taylor, M.A. Reed, *Nano Lett.* 13 (2013) 95.
- [34] C. Xie, B. Nie, L.H. Zeng, L.B. Luo, M. Feng, Y.Q. Yu, C.Y. Wu, Y.C. Wu, S.H. Yu, *ACS Nano* 8 (2014) 4015.
- [35] E.D. Palik, *Handbook of Optical Constants of Solids*, Academic, Orlando, Fla., 1985 (Chap. 2).
- [36] G. Isić, M. Jakovljević, M. Filipović, D. Jovanović, B. Vasić, S. Lazović, N. Puač, Z.L. Petrović, R. Kostić, R. Gajić, J. Humliček, M. Losurdo, G. Bruno, I. Bergmair, K. Hingerl, *J. Nanophoton.* 5 (2011) 051809.
- [37] L.H. Guo, Y. Xu, A.R. Ferhan, G.N. Chen, D.H. Kim, *J. Am. Chem. Soc.* 135 (2013) 12338.
- [38] T.X. Cui, R.T. Lv, Z.H. Huang, S.X. Chen, Z.X. Zhang, X. Gan, Y. Jia, X.M. Li, K.L. Wang, D.H. Wu, F.Y. Kang, *J. Mater. Chem. A* 1 (2013) 5736.
- [39] K.K. Kim, A. Reina, Y.M. Shi, H. Park, L.J. Li, Y.H. Lee, J. Kong, *Nanotechnology* 21 (2010) 285205.
- [40] J.D. Plummer, M.D. Deal, P.B. Griffin, *Silicon VLSI Technology*, Prentice-Hall, Upper Saddle River, NJ, 2000 (Chap. 7).
- [41] H. Haick, P.T. Hurley, A.I. Hochbaum, P.D. Yang, N.S. Lewis, *J. Am. Chem. Soc.* 128 (2006) 8990.
- [42] B. Nie, J.G. Hu, L.B. Luo, C. Xie, L.H. Zeng, P. Lv, F.Z. Li, J.S. Jie, M. Feng, C.Y. Wu, Y.Q. Yu, S.H. Yu, *Small* 9 (2013) 2872.
- [43] E.D. Palik, *Handbook of Optical Constants of Solids*, Academic, Orlando, Fla., 1985 (Chap. 2).



Linbao Luo received M.Sc in inorganic chemistry at Department of Chemistry, University of Science and Technology of China, and Ph.D. degree in 2009 from Department of Physics and Materials Sciences, City University of Hong Kong. After spending 1.5 years at the same university as a senior research associate. He joined the College of Electronic Sciences and Applied Physics, Hefei University of Technology, where he is now a full professor of applied physics. He

has published more than 80 referred journals, with a total citation of ~1800 and an H-index of 24. His research interest mainly focuses on controlled fabrication of one-dimensional semiconductor nanostructures for optoelectronic and electronic devices applications including photovoltaic devices, photodetector, and non-volatile memory device.



Chao Xie received his B.S. and Ph.D. degrees from Hefei University of Technology, China, in 2009 and 2014, respectively. He is currently a research associate in the Department of Applied Physics at the Hong Kong Polytechnic University. His research focuses on the fabrication of novel photovoltaic devices, photodetectors and other electronic/optoelectronic devices based on graphene, silicon nanostructures and II-VI group nanomaterials.



Xian-He Wang received the B.S. degree in physics from the College of Physics, Shandong University of Science and Technology (SUST), in 2012. He is currently a master student in the School of Electronic Science and Applied Physics, Hefei University of Technology. His research interest focuses on the fabrication of surface plasmon resonance enhanced photodetectors based on semiconductor nanostructures.



Yong-Qiang Yu received his B.S. degree in applied physics from Northeastern University, China, and M.S. and Ph.D. degree in Microelectronics and Solid Electronics and Materials Physics and Chemistry from Hefei University of Technology, China, respectively. He is currently a Lecturer at School of Electronic Science and Applied Physics, Hefei University of Technology, China. His current research focuses on the fabrication

and characterization of the nano-devices (such as photodetectors, memories and field effect transistors) and device simulation.



Chun-Yan Wu received her B. Eng. and Master degrees from College of Chemical Engineering, Hefei University of Technology in 1999 and 2004, respectively and Ph.D. degree from the University of Science and Technology of China (USTC) in 2006. She joined the College of Electronic Science and Applied Physics, Hefei University of Technology in 2007. She is currently a visiting scholar to the University of Illinois at

Urbana-Champaign (UIUC), US. Her Research interest include inorganic nanomaterials, nanoelectronic and nanophotovoltaic devices.



Han Hu is currently a master student in the School of Electronic Science and Applied Physics, Hefei University of Technology. He received his B.S. degree in applied physics at Department of Physics, Shandong Normal University, China in 2012. His research focuses on synthesis and transfer of large-area graphene and graphene-based optoelectronic devices.

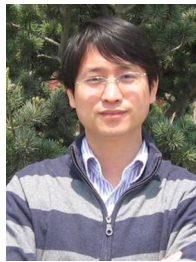


Xi-Wei Zhang received a B.S. and Ph.D. degrees in physics from Harbin Institute of Technology, in 2004 and 2010 respectively. After receiving his PhD degree, he worked as a post-doc in Semiconductor Nano Processing Lab (SNPL), Hanyang University, South Korea. He is currently a lecturer in Department of Physics, Harbin Institute of Technology. His research interest concentrates on optical simulations of nanostruc-

tured solar cells, nonlinear optics, quantum optics, surface plasmon polaritons and related fields.



Ke-Ya Zhou received his B.S. degree from Henan University, M.S. degree from Hefei University of Technology, and Ph.D. degree from Soochow University, in 2008, 2011 and 2014, respectively. He is currently a lecturer in the College of Physics and Electrical Engineering at Anyang Normal University. His research interests include synthesis, controlled doping of II-VI group nanomaterials and their applications as high-performance electronic/optoelectronic devices.



Jiansheng Jie obtained his B.S. and Ph.D. degree in condensed matter physics from University of Science and Technology of China in 1999 and 2004, respectively, and then spent the subsequent three years as a postdoctoral fellow at City University of Hong Kong. He joined the Hefei University of Technology as a professor since 2006. In 2010, he joined the Soochow University, and now his is a professor in the Institute of

Functional Nano & Soft Materials (FUSOM). He is the author or co-author of over 100 research articles in peer reviewed journals with a paper H-index factor of 25. These works have received over 2400 citations. His research interesting includes nanoelectronic and nanooptoelectronic devices, graphene and relevant devices, and solar cells based on silicon nanoarrays.